Wiley Online Library
Early View publication on www.wileyonlinelibrary.com
(issue and page numbers not yet assigned;
citable using Digital Object Identifier – DOI)

Phys. Status Solidi RRL, 1–5 (2014) / DOI 10.1002/pssr.201409032

Part of Focus Issue on
Functional Oxides
Eds.: T. Frauenheim, J. M. Knaup, P. Broqvist, S. Ramanathan

pss +++rapid research letters+++
www.pss-rapid.com

Study of charged defects for substitutionally doped chromium in hexagonal barium titanate from first-principles theory

Sanjeev K. Nayak[*,1], Waheed A. Adeagbo[1], Hans T. Langhammer[2], Wolfram Hergert[1], Thomas Müller[2], and Rolf Böttcher[3]

[1] Institute of Physics, Martin Luther University Halle-Wittenberg, Von-Seckendorff-Platz 1, 06120 Halle, Germany
[2] Institute of Chemistry, Martin Luther University Halle-Wittenberg, Kurt-Mothes-Straße 2, 06120 Halle, Germany
[3] Faculty of Physics and Earth Sciences, Leipzig University, Linnéstraße 5, 04103 Leipzig, Germany

Received 20 January 2014, revised 26 February 2014, accepted 18 March 2014
Published online 24 March 2014

Keywords barium titanate, Cr doping, hexagonal structure, defect formation energy, density functional theory

[*] Corresponding author: e-mail sanjeev.nayak@physik.uni-halle.de, Phone: +49-345-5525439, Fax: +49-345-5525446

We have studied the defect properties of substitutionally doped chromium in hexagonal barium titanate using the density functional theory together with the generalized gradient approximation restricted to exclusively electronic compensation of the charged defect. The supercell used in our studies is large enough to mimic a chromium concentration of about 2 mol%, which corresponds to an amount typically applied in experiments. Chromium is found to prefer the Ti sites inside the face-sharing oxygen octahedra compared with the other non-equivalent Ti sites within the exclusively corner-sharing octahedra of the hexagonal host lattice. Analysis of formation energy, derived from the total energies of defective supercells in various charge states and systematic post-processing, shows that the charge state of –1 is stable for wide range of Fermi energy within the band gap. The charge state of 0 is only stable for a very low electron concentration, i.e. for highly oxidizing conditions.

1 Introduction Semiconductor defects have been a long studied topic which is attractive because of the tunability of physical properties of host semiconductors and thus have found direct applications in the form of electronic devices as we know it today. In this field, barium titanate (BTO) is the prototype material for ferroelectric applications. If ferromagnetic properties are incorporated by engineering that material, e.g., with 3d transition metals (TM), such type of multiferroic material could be potentially important for spintronics technology [1]. Despite this fact, only few *ab initio* based studies on the electronic structure of BTO with point defects have been published in the past, although pure BTO and its surfaces are still a matter of interest [2]. For example, Michel–Calendini and Moretti investigated the incorporation of Cr, Mn, and Co on the Ti site by the self-consistent-field Xα spin-unrestricted method [3, 4]. Their investigations and by far most of other *ab initio* calculations are related to the cubic or tetragonal structure of BTO. There is a lack of first-principle calculations for the high-temperature hexagonal modification of BTO which can be stabilized at room temperature by doping with most of the 3d transition metals at concentrations in the order of 1 mol% [5]. Till now, *ab initio* calculations of the electronic structure of hexagonal BTO by density functional theory (DFT) are known only for undoped [6, 7], Ru-doped [6] and Co-doped [8] material. But generally, a more detailed study regarding the atomistic features in doped hexagonal BTO is missing.

Hence, in the present work, we undertake *ab initio* DFT calculations for the study of Cr doped BTO with a concentration of approx. 2 mol%, which is found to be in hexagonal phase at room temperature [9, 10]. The hexagonal BTO structure, shown in Fig. 1, consists of two inequivalent atoms of each component, which are called

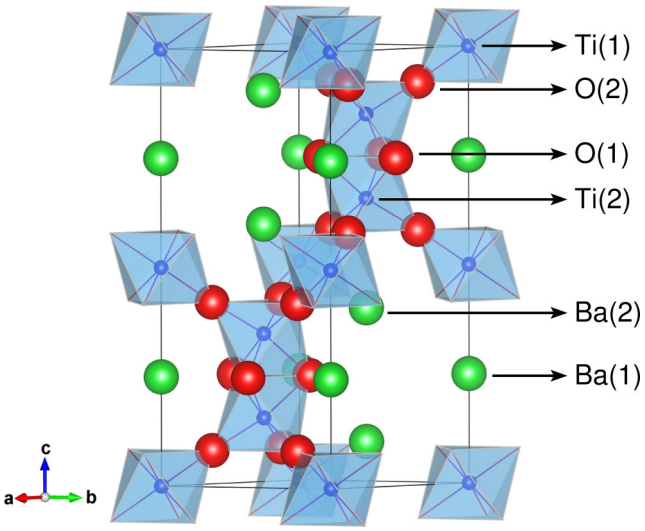

Figure 1 Schematic representation of the primitive cell of hexagonal (6H-type) barium titanate. It consists of six $BaTiO_3$ stoichiometric units (30 atoms). The green, blue and red balls represent the Ba, Ti and O atoms, respectively. For clarity, only the oxygen atoms belonging to the primitive cell are shown.

Ba(1), Ba(2), Ti(1), Ti(2), O(1) and O(2). The different positions of Ti(1) and Ti(2) are related to the two non-equivalent oxygen octahedra of the hexagonal structure. Whereas Ti(1) is surrounded by 6 oxygen atoms of the exclusively corner-sharing octahedra, Ti(2) is located inside the face-sharing, trigonally distorted octahedra.

Recent experimental studies of chromium doped, air-sintered hexagonal BTO ceramics using electron paramagnetic resonance (EPR) as the main method have suggested that Cr is incorporated at Ti sites both as Cr^{3+} (lattice charge state –1) and as Cr^{4+} (neutral charge state) [9, 10]. Additionally, it was found that Cr^{3+} prefers the Ti(2) site at lower concentrations. Despite these experimental findings we have investigated the probability of site occupancy of substitutional Cr on both Ti and Ba sites in order to avoid *a priori* exclusion of certain incorporation sites, since it is known that 3d TM atoms, e.g. Ni can enter the Ba site of BTO [11]. In addition, the stability of the neutral (Cr^{4+}) and different non-zero charge states of Cr were investigated. The latter states need a suitable mechanism for charge compensation, which will be decisive for the material properties. For example, charge compensation achieved by additional electrons in the conduction band (holes in the valence band) for positively (negatively) charged defects will induce different transport properties than in cases where the charge compensation is achieved by additional intrinsic or extrinsic atomic point defects in the sample. In the present study we restrict to substitutionally doped Cr on Ti and Ba sites and explore the stability of charged Cr states for exclusively electronic charge compensation.

2 Computational details

2.1 Density functional calculations Total energy calculations with spin polarized DFT are performed by using the plane-wave pseudopotentials code Vienna *ab initio* simulation package (VASP) [12, 13]. The 5s5p6s, 3p3d4s, 2s2p, and 3p3d4s states are treated as the valence states for the atomic pseudopotentials of Ba, Ti, O and Cr, respectively, together with the projector augmented-wave treatment [14]. The generalized gradient approximation for the exchange-correlation functional in the parameterization of Perdew and Wang [15] is used for the calculations. The kinetic energy cutoff for the plane waves is set to 400 eV. A supercell of $3 \times 3 \times 1$ times periodic repetition of the primitive hexagonal cell, containing 270 atoms in total, is used for the defect calculations. In the substitutional defect study, one of the Ti or Ba atoms is replaced by a Cr atom. This corresponds to a defect concentration of 1.85 mol%. For the charged calculations, the negative or positive charge states are achieved by adding or removing integral numbers of electrons, respectively, to or from the supercell. In order to preserve the charge neutrality of the supercells, a compensating homogeneous background charge is introduced in the calculations of charged defects. The supercell is relaxed in order to minimize the internal strain due to the impurity atoms until the residual forces on each atom is below 25 meV/Å. The density of states is generated with $3 \times 3 \times 3$ Γ-centered Monkhorst–Pack k-points grid using the tetrahedron method. The change in total energy obtained by increasing the k-points grid to $5 \times 5 \times 5$ is negligibly small, thus the total energies obtained from $3 \times 3 \times 3$ k-points grid are taken for analysis.

2.2 Formation energy of point defects In order to compare the stability of charged defects we have calculated the formation energy of Cr_{Ti} and Cr_{Ba} defects with different supercell charges. The formation energy is calculated as

$$E_{\mathrm{For}}(D,q) = E(D,q) - E(\mathrm{BTO}) + \sum_i n_i \mu_i + q(E_{\mathrm{V}} + \Delta E_{\mathrm{F}}) + \Delta E_{\mathrm{PP}}, \quad (1)$$

where $E_{\mathrm{For}}(D,q)$ and $E(D,q)$ are the formation energy and total energy of the point defect D with supercell charge q, respectively. E(BTO) is the total energy of host supercell containing equivalent number of atoms as that of the defect supercell. The growth conditions for the crystal are incorporated through the chemical potentials (μ_i) of the elemental species with the number n_i of atoms added (n_i negative) or removed (n_i positive) from the pure host semiconductor. The Fermi level is referenced with respect to the valence band maximum (E_{V}) and is related to E_{V} as $E_{\mathrm{F}} = E_{\mathrm{V}} + \Delta E_{\mathrm{F}}$. Thus, ΔE_{F} has a range from zero to the band gap (E_g), since usually $E_{\mathrm{V}} < E_{\mathrm{F}} < E_{\mathrm{C}}$ (conduction band minimum) is the region of interest for semiconductors. ΔE_{PP} is a set of post-processing corrections for the formation energy which is discussed in the next section.

2.3 Post-processing of the DFT results The formation energies as obtained from the DFT calculations have several shortcomings. It has been emphasized by Lany and Zunger in their critical assessment that post-processing of the formation energies (computed with the GGA) must be carried out in order to interpret the physics of defects correctly [16]. The different corrections which are put together into one term ΔE_{PP} in the formation energy of Eq. (1) is written as

$$\Delta E_{PP} = q\left(\Delta E_V + (1+f)\left[\frac{q\alpha_M}{2\varepsilon L}\right] + (V^r_{D,q} - V^r_H)\right) - \sum_{n,\boldsymbol{k}} \omega_{\boldsymbol{k}} \eta_{n,\boldsymbol{k}} (e_{n,\boldsymbol{k}} - \tilde{e}_C)\,\Theta(e_{n,\boldsymbol{k}} - \tilde{e}_C) + z_e\,\Delta E_C - z_h\,\Delta E_V, \quad (2)$$

where ΔE_V and ΔE_C are the relative shifts of the valence band and conduction band edges, respectively. This is estimated by comparing the electronic structure obtained from GGA and GGA + U methods (U = 5.0 eV on Ti d-orbitals [17]) and extrapolating it to get the experimental E_g of host semiconductor. The value of E_g were obtained as 1.73 eV and 2.28 eV, respectively, from GGA and GGA + U methods. The experimental E_g was taken to be 3.40 eV. We obtained the values of 0.429 eV and 2.103 eV for ΔE_V and ΔE_C, respectively.

The variables α_M, ε, and L are the Madelung constant, dielectric constant and the size of the supercell ($L = \sqrt[3]{V}$, where V is volume of the supercell), respectively. The value for α_M = 62.95 is taken from Ref. [18] and the value of ε is set to 57 as used in Ref. [7]. It has been shown in Ref. [16] that the proportionality factor for the image charge correction for a finite supercell (f) range from the value of –0.34 to –0.37, depending on the crystal structure. Owing to the fact that cubic close-packed structures (fcc) and hexagonal close-packed structures (hcp) have similar packing densities, the value of f for the hexagonal BTO lattice is taken as –0.34, as holds for the fcc lattice.

The summand $V^r_{D,q}$ is the average electrostatic potential over a sphere around an atomic site far from the defect and V^r_H is the corresponding average electrostatic potential of the same site in the host supercell. The difference between $V^r_{D,q}$ and V^r_H is taken into account in order to align the potential of defect supercell to that of the host supercell. It must be emphasized that owing to the crystal symmetry, we obtained different average electrostatic potentials for Ti(1) and Ti(2) sites (similarly also for Ba and O). Thus, in order to analyze, for example, Cr substituting Ti(2), we align the potential by comparing the average electrostatic potential of Ti(1) laying at a position far away from the impurity site.

The Moss–Burstein type band filling effects which might appear due to finite size of supercell (thereby large concentration of defects) are corrected by the term consisting of summation over the bands n and the k-points as shown in Eq. (2). The variables associated with this correction term, namely, $\omega_{\boldsymbol{k}}$, $\eta_{n,\boldsymbol{k}}$ $e_{n,\boldsymbol{k}}$ and $\tilde{e}_C$ are the k-point weight, band occupation, band energies of defect supercell and the conduction band edge of pure host (after the potential alignment is done as stated above). Θ is the Heaviside step function. This correction term gives almost zero values for Cr_{Ti} defects, but is not negligible for Cr_{Ba} defects in the charge state 0 and –1.

Finally, the correction term in order to account for the shift of shallow levels with respect to the host band edges is calculated by adding (subtracting) the product of number of electrons z_e (number of holes z_h) and the shift in band level ΔE_C (ΔE_V) as shown in Eq. (2). Here, z_e (similarly z_h) is obtained by integrating the total density of electronic states suitably.

There remains an open question relating to how the deep defects must be corrected. A linear extrapolation of deep defect levels by comparing the GGA and GGA + U electronic structure have been reported [19–21]. However, we find that such a correction contributed large values in the formation energy ranging from 1–7 eV, depending on the charge state, as compared to the formation energy computed from the GGA total energies together with the discussed postprocessing procedure. Such changes are unphysical since the corresponding formation energies are far from any reasonable prediction for Cr defects in BTO.

3 Results and discussion DFT calculations are performed for Cr substituted on the two inequivalent positions ((1) and (2)) of the cation M (M = Ba and Ti) in BTO. The total-energy difference between the site occupancies for the respective defect is calculated as

$$\Delta E_{site} = E(Cr_{M(1)}) - E(Cr_{M(2)}). \quad (3)$$

A positive value of ΔE_{site} implies that the M(2) site is more preferential than the M(1) site and vice versa. For both Ba and Ti, it is observed that the site (2) is more likely for Cr substitution than the site (1). This is because the (2) site is surrounded by six oxygen atoms which have relatively smaller M(2)–O bond lengths than the M(1)–O bond lengths, thus making it chemically more stable. The energy difference ΔE_{site} obtained for different charged states for $E(Cr_{Ti})$ is shown in Table 1.

Table 1 Energy differences (in eV) between supercells with site occupancies of Cr on inequivalent sites (1) and (2) for M = Ti, as shown in Eq. (3), and the corresponding magnetic moments of Cr ($m(Cr_{Ti})$) in μ_B are tabulated. The location of Fermi level (E_F) in the density of states (in band gap (BG) or in conduction band (CB)) is also tabulated.

q	ΔE_{site}	$m(Cr_{Ti(1)})$	$m(Cr_{Ti(2)})$	E_F
–2	0.1073	2.574	2.523	CB
–1	0.3202	2.581	2.527	BG
0	0.8335	1.845	1.800	BG
+1	0.8526	0.975	0.933	BG

Table 1 also shows the magnetic moment m of Cr at the Ti(1) and Ti(2) sites for different charge states obtained in our calculations. The magnetic moment of Cr_{Ti} varies roughly as 1, 2 and 2.5 μ_B/Cr for the charge states +1, 0 and –1, respectively. This suggests that with addition of electrons into the system, the electrons are tendentially less localized on the Cr atoms. This is clearly seen as we go from $q = 0$ to $q = -1$. Moreover, by adding one electron to state $q = -1$ leading to $q = -2$, we find that the magnetic moment does not change. This shows that below a specific value of q, the added electrons are no more localized on Cr and thus are found in the conduction band. The location of the Fermi level obtained from the density of states is shown in the fourth column of Table 1. It is observed that while for charge states +1, 0 and –1 the Fermi level lies in the band gap (BG), for the charge state –2 it lies in the conduction band (CB).

The formation energy (E_{For}) plotted against the Fermi level position relative to E_V for different charge states of Cr_{Ti} and Cr_{Ba} defects are shown in Fig. 2. The chemical potentials for the E_{For} calculated according to Eq. (1) are derived for O-rich and Ti-poor conditions which are often encountered in experiments. The chemical potentials μ_{Ba}, μ_{Ti}, and μ_{Cr} are taken from the total energies of BaO, TiO_2, and Cr_2O_3, respectively. The E_V obtained from a regular GGA calculation (E_V (GGA)) and that obtained after post-processing (E_V (fixed)) are shown as vertical dashed line and vertical solid line on the left-hand side of the plot. The solid vertical line on the right-hand side of the plot represents the experimental band gap with respect to the E_V (fixed).

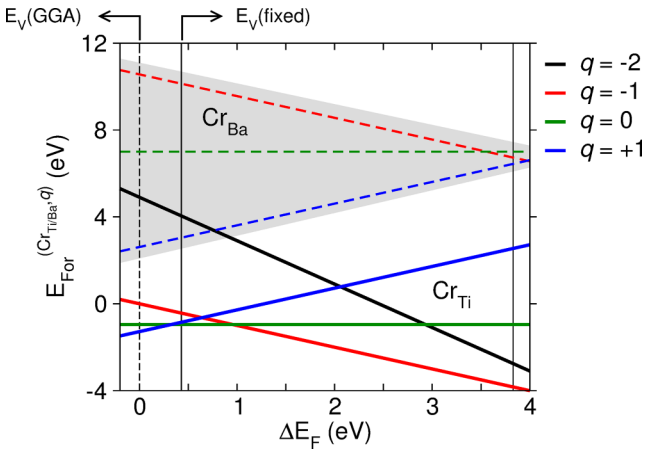

Figure 2 Formation energy of charged defects as a function of Fermi level position relative to E_V. The left dashed and solid vertical lines are the valence band maxima obtained from GGA (E_V(GGA)) and after post-processing (E_V(fixed)) as discussed in text. The solid vertical line on the right-hand side of the plot marks the experimental band gap measured from E_V(fixed). The formation energy of Cr_{Ba} defects (shown as dashed lines) are bounded by a shaded region in order to differentiate between formation energies of Cr_{Ti} defects. The charge state of +1 is stable for Cr_{Ba}, while both $q = 0$ and $q = -1$ are found for Cr_{Ti} with the transition level (q = 0/–1) occurring at 0.52 eV above the E_V (fixed).

The formation energy shown in Fig. 2 suggests that the Cr_{Ti} defect is more favorable than the Cr_{Ba} defect (shown as dashed lines in the grey region) for all the charge states. Except in the region close to E_V (fixed) (representing strongly oxidizing environment), where the charge state $q = 0$ is stable, for most regions of ΔE_F the charge state $q = -1$ is found to be more stable. The charge transition level ($q = 0/-1$) for Cr_{Ti} is found to be 0.52 eV above the E_V (fixed), which remains to be verified experimentally. The finding that the charge state $q = 0$ (corresponds to Cr^{4+}) is stable only in highly oxidizing environment during crystal growth seems to be reasonable.

The disadvantage of referencing the formation energy with respect to the E_V (GGA) is quite apparent in our studies. When referenced from E_V (GGA), it is observed that for very low electron concentration (i.e. ΔE_F close to E_V (GGA)) the $q = +1$ has lower formation energy than the $q = 0$ state. However, this contradicts the general properties of Cr doped BTO as observed in experiments. In fact, this difficulty is overcome by considering the referencing from E_V (fixed) as suggested in Ref. [16], thus affirming the band edge correction scheme.

4 Summary and outlook The defect physics of Cr doped BTO is studied for the hexagonal structure using density functional theory. Out of the two types of substitutional defects considered, Cr_{Ti} and Cr_{Ba}, the formation energy shows that Cr_{Ti} is definitely more probable because of lower formation energy than Cr_{Ba}. The total energy analysis for the site occupancy shows that the inequivalent site (2) is more favorable than site (1) for both Ti and Ba owing to smaller bond lengths of the impurity Cr at site (2) with the neighboring oxygen atoms.

We have considered only the charge compensation by electronic mechanisms for the defect studies. However, charge compensation by other point defects might be potentially competing with the electronic mechanism. For example, oxygen vacancies are often found in acceptor-doped oxide semiconductors, which can strongly influence the properties of the host semiconductor. Some of our studies are ongoing in order to understand the influence of oxygen vacancies on the properties of Cr doped BTO.

Acknowledgements The work is funded by the Deutsche Forschungsgemeinschaft through the Collaborative Research Center SFB 762 “Functionality of Oxide Interfaces”. One of the authors (SKN) would like to thank Prof. Alex Zunger for discussions on the defect studies. The computational support from Universitätsrechenzentrum, Martin Luther University Halle-Wittenberg is also acknowledged.

References

[1] J. Y. Son, J.-H. Lee, S. Song, Y.-H. Shin, and H. M. Jang, ACS Nano **7**, 5522 (2013).
[2] R. I. Eglitis and D. Vanderbilt, Phys. Rev. B **76**, 155439 (2007).

[3] F. M. Michel-Calendini and P. Moretti, Phys. Rev. B **27**, 763 (1983).
[4] P. Moretti and F. M. Michel-Calendini, Phys. Rev. B **36**, 3522 (1987).
[5] S. Jayanthi and T. Kutty, J. Mater. Sci.: Mater. Electron. **19**, 615 (2008).
[6] T. A. Colson, M. J. Spencer, and I. Yarovsky, Comp. Mater. Sci. **34**, 157 (2005).
[7] J. A. Dawson, J. H. Harding, H. Chen, and D. C. Sinclair, J. Appl. Phys. **111**, 094108 (2012).
[8] Y. Li, Q. Liu, T. Yao, Z. Pan, Z. Sun, Y. Jiang, H. Zhang, Z. Pan, W. Yan, and S. Wei, Appl. Phys. Lett. **96**, 091905 (2010).
[9] R. Böttcher, E. Erdem, H. T. Langhammer, T. Müller, and H.-P. Abicht, J. Phys.: Condens. Matter **17**, 2763 (2005).
[10] H. T. Langhammer, T. Müller, R. Böttcher, and H.-P. Abicht, J. Phys.: Condens. Matter **20**, 085206 (2008).
[11] S. Lenjer, R. Scharfschwerdt, T. Kool, and O. Schirmer, Solid State Commun. **116**, 133 (2000).
[12] G. Kresse and J. Furthmüller, Comp. Mater. Sci. **6**, 15 (1996).
[13] G. Kresse and J. Furthmüller, Phys. Rev. B **54**, 11169 (1996).
[14] G. Kresse and D. Joubert, Phys. Rev. B **59**, 1758 (1999).
[15] J. P. Perdew, in Electronic Structure of Solids, edited by P. Ziesche and H. Eschrig (Akademie Verlag, Berlin, 1991), pp. 11–20.
[16] S. Lany and A. Zunger, Phys. Rev. B **78**, 235104 (2008).
[17] D. D. Sante, K. Yamauchi, and S. Picozzi, J. Phys.: Condens. Matter **25**, 066001 (2013).
[18] A. Sabry, M. Ayadi, and A. Chouikh, Comp. Mater. Sci. **18**, 345 (2000).
[19] A. Janotti and C. G. Van de Walle, Phys. Rev. B **76**, 165202 (2007).
[20] A. Janotti and C. G. Van de Walle, Phys. Status Solidi B **248**, 799 (2011).
[21] E. Ertekin, V. Srinivasan, J. Ravichandran, P. B. Rossen, W. Siemons, A. Majumdar, R. Ramesh, and J. C. Grossman, Phys. Rev. B **85**, 195460 (2012).